Original papers
Nanostructured, nanoscale materials and nanodevices

УДК 546.824;665.7.035.8 DOI: 10.17277/jamt.2022.01.pp.068-077

Synthesis and dielectric properties of $K_{1.6}Fe_{1.6}Ti_{6.4}O_{16}$ ceramics produced by the Pechini method

Alexey R. Tsyganov[a] ✉, Alexander V. Gorokhovsky[a], Maria A. Vikulova[a], Denis I. Artyukhov[a], Dmitry A. Zakharievich[b], Svetlana I. Saunina[b], Nikolay V. Gorshkov[a]

[a] *Yuri Gagarin State Technical University of Saratov, 77, Polytechnicheskaya St., Saratov 410054, Russian Federation,*
[b] *Chelyabinsk State University, 129, Br. Kashirinykh St., Chelyabinsk 454001, Russian Federation*

✉ tsyganov.a.93@mail.ru

Abstract: Potassium titanate modified with Fe^{3+} ions matching the stoichiometry of $K_{1.6}Fe_{1.6}Ti_{6.4}O_{16}$ (KFTO) was obtained by the polymer complex precursor method (Pechini method). The phase composition and morphology of the obtained sample were characterized using XRD, laser diffraction, and SEM technique. X-ray phase analysis shows single-phase formation of potassium titanate with a tetragonal hollandite-like structure. The Rietveld method was used to clarify the crystal lattice parameters. The parameters of the crystal lattice are: $a = b = 10.1510$ Å и $c = 2.9659$ Å. The results of SEM and laser diffraction showed that the particles of the studied nanopowder have a cubic shape and an average size of 400 nm. The dielectric properties in the frequency range of 0.1 Hz to 1.0 MHz were studied for ceramic disks obtained by sintering of compressed nanopowder at 1080 °C. It was found that ceramics based on KFTO solid solutions have high dielectric permittivity and low dielectric losses and characterized with increased polarizability. The high polarizability of the material is explained by the relatively high mobility of K^+ ions in the tunnel of the considered hollandite structure that is accompanied by the redistribution of electrons in the crystal lattice. A discussion of the contribution of various processes to the permittivity is presented.

Keywords: hollandite structure; Pechini method; ceramic; impedance; dielectric properties; permittivity; dielectric losses; nanopowder.

For citation: Tsyganov AR, Gorokhovsky AV, Vikulova MA, Artyukhov DI, Zakharievich DA, Saunina SI, Gorshkov NV. Synthesis and dielectric properties of $K_{1.6}Fe_{1.6}Ti_{6.4}O_{16}$ ceramics produced by the Pechini method. *Journal of Advanced Materials and Technologies*. 2022;7(1):68-77. DOI: 10.17277/jamt.2022.01.pp.068-077

Синтез и диэлектрические свойства $K_{1.6}Fe_{1.6}Ti_{6.4}O_{16}$ керамики, полученной методом Печини

А. Р. Цыганов[a] ✉, А. В. Гороховский[a], М. А. Викулова[a], Д. И. Артюхов[a], Д. А. Захарьевич[b], С. И. Саунина[b], Н. В. Горшков[a]

[a] *Саратовский государственный технический университет имени Гагарина Ю. А., ул. Политехническая, 77, Саратов 410054, Российская Федерация,*
[b] *Челябинский государственный университет, ул. Братьев Кашириных, 129, Челябинск 454001, Российская Федерация*

✉ tsyganov.a.93@mail.ru

Аннотация: Титанат калия, модифицированный ионами Fe^{3+} и соответствующий стехиометрии $K_{1.6}Fe_{1.6}Ti_{6.4}O_{16}$ (KFTO), получен методом полимерных комплексов прекурсоров (метод Печини). Фазовый состав, распределение частиц по размеру и морфология образцов полученных материалов были охарактеризованы методами рентгенофазового анализа (РФА), дифракции лазерного излучения и СЭМ. Рентгенофазовый анализ показывает однофазное образование титаната калия с тетрагональной структурой голландита. Для уточнения параметров кристаллической решетки использован метод Ритвельда. Параметры решетки составляют: $a = b = 10{,}151$ Å и $c = 2{,}9659$ Å. Результаты СЭМ и дифракции лазерного излучения показали, что частицы исследуемого нанопорошка имеют кубическую форму и средний размер 400 нм. Диэлектрические свойства в диапазоне частот 0,1 Гц до 1,0 МГц исследованы для керамических дисков, полученных методом спекания, спрессованного

нанопорошка при 1080 °C. Установлено, что керамика на основе твердых растворов KFTO обладает высокой диэлектрической проницаемостью и низкими диэлектрическими потерями и характеризуется повышенной поляризуемостью структуры. Высокая поляризуемость материала объясняется относительно высокой подвижностью ионов K^+ в туннеле рассматриваемой структуры голландита, сопровождающейся перераспределением электронов в кристаллической решетке. Приведено обсуждение вклада различных процессов в диэлектрическую проницаемость.

Ключевые слова: структура голландита; метод Печини; керамика; импеданс; диэлектрические свойства; диэлектрическая проницаемость; диэлектрические потери; нанопорошок.

Для цитирования: Tsyganov AR, Gorokhovsky AV, Vikulova MA, Artyukhov DI, Zakharievich DA, Saunina SI, Gorshkov NV. Synthesis and dielectric properties of $K_{1.6}Fe_{1.6}Ti_{6.4}O_{16}$ ceramics produced by the Pechini method. *Journal of Advanced Materials and Technologies*. 2022;7(1):68-77. DOI: 10.17277/jamt.2022.01.pp.068-077

1. Introduction

As a result of accelerated development of electronics, the materials with high dielectric permittivity and low dielectric losses and high structural stability are increasingly in demand. Among these materials, ceramic materials with perovskite structure have become a popular research topic due to their satisfactory dielectric properties and versatility [1]. In recent decades, $BaTiO_3$ has become the most successfully commercialized dielectric material for electronic devices such as capacitors, converters and sensors due to its excellent dielectric, ferroelectric and piezoelectric properties [2–5]. Special mention should be paid to miniature multilayer ceramic capacitors (MLCC) [6]. With their good frequency response, higher reliability, high breakdown voltage, superior volumetric capacitance efficiency and reduced cost, MLCC with $BaTiO_3$ ferroelectric compositions are already competing with conventional high-capacity Al- or Ta-electrolytic capacitors. In applications such as mobile electronic equipment (cell phones or laptops), these MLCC types dominate at present and will also play an important role in the future [7]. This one is related to their excellent dielectric properties such as high polarization, high dielectric constant ($\varepsilon = 3600$ at 25 °C and at 100 kHz) and relatively low dielectric losses ($\tan\delta = 0.032$). In addition to barium titanate, last decade, ceramics of the composition $CaCu_3Ti_4O_{12}$, characterized with a colossal dielectric constant (CDC), are of great interest too [8–10]. However, CCTO ceramics have high tan(δ) values that limit its practical application. In this regard, the development and study of various oxide systems with high permittivity is an urgent task [11].

Complex oxides $K_x(Me,Ti)_8O_{16}$ with hollandite structure [12, 13] can be considered as new materials with high permittivity. Hollandite family can be represented by the general formula $A_xB_8O_{16}$, where A are tunnel cations, B are octahedral cations. The elementary cell $A_xB_8O_{16}$ can have different occupancy of tunnel cations ($0 \le x \le 2$). The cations are usually represented by groups of univalent alkali and divalent alkaline earth metals, such as K^+, Na^+, Li^+, Ba^{2+}, etc.; and B cations can be represented by different metals or transition elements with different sizes and oxidation degrees, such as Ti^{3+}, Ti^{4+}, Mg^{2+}, Fe^{2+}, Ni^{2+}, Al^{3+}, Fe^{3+}, Sn^{4+} etc. Depending on the average sizes of A and B cations, hollandite can have tetragonal (I4/m) or monoclinic (I2/m) symmetry with tunnels along the crystallographic c or b axis, respectively [14–16]. Hollandite-like materials are outstanding representatives of tunnel oxides with a wide range of applications, including anode materials for solid-state batteries [17], carrier grids for radionuclide removal [18], etc. In the last decade, it has been noted that a group of oxide materials characterized by a tunnel structure similar to hollandite has been characterized by enormous permittivity [19, 20]. As shown in [19], the $K_{1.53}Cu_{0.76}Ti_{7.24}O_{16}$ copper-doped hollandite-like potassium titanate was obtained by treating the amorphous potassium polytitanate with aqueous solutions of copper sulfate followed by calcination at 900 °C. These materials were found to have a high permittivity ($\varepsilon = 2000$, $\delta = 0.6$ at 25 °C, at 1 kHz). In addition it is shown [21] that hollandite-like solid solutions are promising ceramic fillers for polymer-matrix composites due to their stable and high value of permittivity. It is important to note that the replacement of some Ti^{4+} positions by divalent or trivalent transition metals, which promotes the formation of hollandite-like solid solutions $K_x(Me,Ti)_8O_{16}$, contributes to an increase in polarization ability and permittivity [20]. Although the crystal structure of the hollandite-like materials has been studied in detail, no systematic approach has yet been undertaken to study the dielectric properties of this material class.

The main methods to produce the hollandite-like ceramics are: solid-state reactions [19–22], sol-gel method [23–26] and hydrothermal synthesis [27]. The disadvantages of these methods include: high

synthesis temperature, long reaction time, low control of stoichiometric composition, and large particle sizes. For this reason, exploring new ways to synthesize this material is very important to guaranty the required stoichiometry, minimum content of secondary phases and particle size, as well as controlled morphology, necessary to improve material properties for its applications. For such systems, the Pechini method is applicable [28–30], where the synthesis takes place by forming a polymeric precursor in which the metal ions of interest are evenly distributed along the macromolecular chains produced by esterification and polymerization reactions between citric acid and ethylene glycol. The advantages of this method include a possibility to obtain nanopowders with high control of stoichiometry and purity, low synthesis temperatures and high reproducibility. In addition, the resulting powders do not require a use of the additional milling for further fabrication of ceramic products with low porosity.

The hollandite composition similar to $K_{1.6}Fe_{1.6}Ti_{6.4}O_{16}$ was previously obtained in works [12, 24], but so far there have been no studies of ceramic dielectric properties in this class of materials. In addition, iron ions have a variable valence, which can lead to an increase in polarization of the dielectric and increase its permittivity. In this connection, a study of iron-containing material with a hollandite structure is of scientific and practical interest. As part of this study, a modified sol-gel method with the addition of ethylene glycol was successfully tested, which promotes the polymerization of chelates and reduces the ion mobility during the synthesis. The use of this synthesis method made it possible to obtain a pure structure of hollandite without impurity phases. This study for the first time contains the results of a study of the dielectric properties of $K_{1.6}Fe_{1.6}Ti_{6.4}O_{16}$ in a wide frequency range, a detailed description of impedance spectroscopy data indicating the processes occurring in the grain and at the grain boundary, an equivalent scheme is proposed and the corresponding parameters were calculated.

Thus, the aim of this paper was to obtain a solid solution with the general formula of $K_{1.6}Fe_{1.6}Ti_{6.4}O_{16}$ (KFTO) by the Pechini method and study the dielectric properties of the ceramics based thereon.

2. Materials and methods

2.1. Synthesis of $K_{1.6}Fe_{1.6}Ti_{6.4}O_{16}$

Precursor materials used for the synthesis of nanopowders in the K_2O–TiO_2–Fe_2O_3 system were ethylene glycol (99 %, Russian Standard 10164–75), citric acid (99.8 %, Russian Standard 3652–69), KNO_3 (98 %, Russian Standard 4217–77), $Fe(NO_3)_3 \times \times 9H_2O$ (98 %, TC 6-09-02-553-96), $C_{16}H_{36}O_4Ti$ (97 %, Aldrich), HNO_3 (65 %, Russian Standard 4461–77), aqueous ammonia (25 %, Russian Standard 3760–79).

The methodology of nanopowders producing included several steps. Nitrates of the corresponding metal ions were dissolved in a minimal amount of distilled water, and then added to titanium butoxide in stoichiometric ratios corresponding to $K_{1.6}Fe_{1.6}Ti_{6.4}O_{16}$. An aqueous solution of nitric acid, citric acid, and ethylene glycol were added to the resulting mixture. Optimal stoichiometric ratios were determined experimentally in advance $Ti : C_6H_8O_7 = 1.5$; $Ti : C_2H_6O_2 = 5.5$; $Ti : NO_3 = 1.8$. After titanium butoxide was completely dissolved, a 10 % NH_4OH solution was added to the solution until $pH = 8$ was established. According to the Pechini method, the next step was made to evaporate the solvent and support polymer resin formation in a drying oven at 240 °C to initiate a self-sustaining combustion reaction and provide extraction of the released NO_2. The gel first underwent melting, then boiling, and then swelled into black foam, which finally burst into flames and burned to black ash. The combustion continued for several minutes with a smoldering flame. The resulting amorphous ash was annealed at 900 °C in an electric furnace for 20 minutes to produce crystalline nanopowders.

2.2. Characterizations

To study the dielectric properties, the KFTO powder was pressed in a stainless steel mold at 150 MPa (disk diameter 12 mm, thickness 1 mm) and sintered at 1080 °C to form monolithic ceramic bodies. The obtained ceramic discs were coated with silver-palladium adhesive (Trademark K13, Russia).

The phase composition of the ceramic material was studied using the X-ray diffractometer Thermo Scientific ARL X'TRA (Cu K_α radiation, $\lambda = = 0.15412$ nm). The morphology of the samples was analyzed using the scanning electron microscope Vega3 Tescan. The fractional composition of the obtained powders was studied using the laser particle size analyzer Analysette 22 MicroTecplus (Fritsch), recalculation of the experimental data was performed in the MaScontrol software using the Fraunhofer theory. Raman spectra were acquired from powder samples using a Bruker Raman microscope, scanning with a green laser of wavelength 514 nm in the range from 250 to 2000 cm^{-1}. The measurement of the

electrical properties of the obtained ceramic disks were determined by impedance spectroscopy (Novocontrol Alpha AN impedance analyzer) in the frequency range from 0.1 Hz to 1.0 MHz at a voltage amplitude of 100 mV.

3. Results and discussion

Figure 1*a* shows the XRD patterns of the synthesized KFTO specimens. As can be seen, all the reflexes fully correspond to pure KFTO with a tetragonal hollandite-like structure (spatial group I4/m, JCPDS No. 77- 0990). It is worth noting the absence of impurity crystal structures, such as Fe_2O_3, $FeTiO_3$, which confirms the replacement of titanium with iron injected during the synthesis. For the sample sintered at 1080 °C, the diffractogram shows a presence of the Fe_2TiO_5 reflexes. The formation of Fe_2TiO_5 crystals on the grain boundaries can be considered as a result of oxygen loss from the grain mass during high-temperature sintering and diffusion of iron from the bulk of the grains to their boundaries, as well as subsequent re-oxidation during cooling of sintered ceramics [31–33].

The structure of the synthesized hollandite-like ceramics is shown in Fig. 1*b*. The KFTO structure of the hollandite consists of interconnected $(Fe,Ti)O_6$ octahedrons forming a framework with tunnels filled with K^+ ions (the potassium ions displacement is shown by purple sectors in Fig. 1*b*). Titanium ions have a mixed valence +4 (dark colored atoms in the center of octahedrons) or +3 (light colored atoms in the center of octahedrons) and can be replaced by ions of various transition metals, such as Fe^{3+} in this case.

Figure 1*c* shows a typical plot of the final Rietveld refinement, indicating a good match between the experimental and calculated intensities in the tetragonal system with spatial group I4/m. The factors of the final convergence agreement are satisfactory: $R_p = 12.86$ %, $R_{wp} = 17.36$ %. The calculated parameters of the lattice are $a = b = 10.151$ Å and $c = 2.9659$ Å, theoretical density (d_{theor}) 3.86 g·cm^{-3}. Calculated convergence factor GOF = 4.03. The cell constants are in fairly good agreement with comparable compositions of priderites, taking into account the ionic radii of the doping metals [12].

Figure 2 shows the particle size distribution and the SEM micrograph of the obtained ceramic powder. As can be seen, the particles are characterized by uncertain morphology and an average size of 400 nm.

Using literature data on Raman bands characteristic of titanates and experimental results (Fig. 3), we correlated the Raman bands of our samples with different types of vibrations of their constituent elements. The 375 cm^{-1} band, for a compound with a tunneling Hollandite-like structure of $K_{1.6}Fe_{1.6}Ti_{6.4}O_{16}$ composition, probably corresponds to the strain vibrations of $(Fe,Ti)O_6$ octahedrons. The 449 cm^{-1} band corresponds to Ti–O vibrations in a one-dimensional channel of hollandite structure.

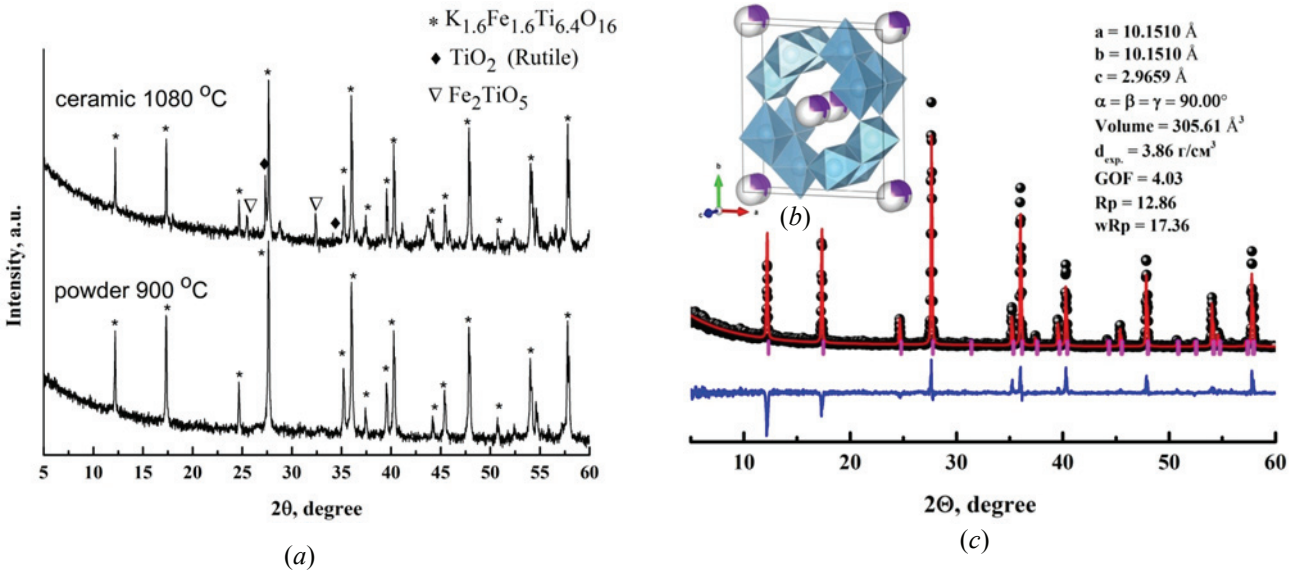

Fig. 1. X-ray pattern (*a*) of the powder KFTO sample; (*b*) crystal structure of hollandite-type KFTO; (*c*) the refined Rietveld plot showing experimental (black ball), calculated (red line) and difference (blue line) for priderite powder KFTO

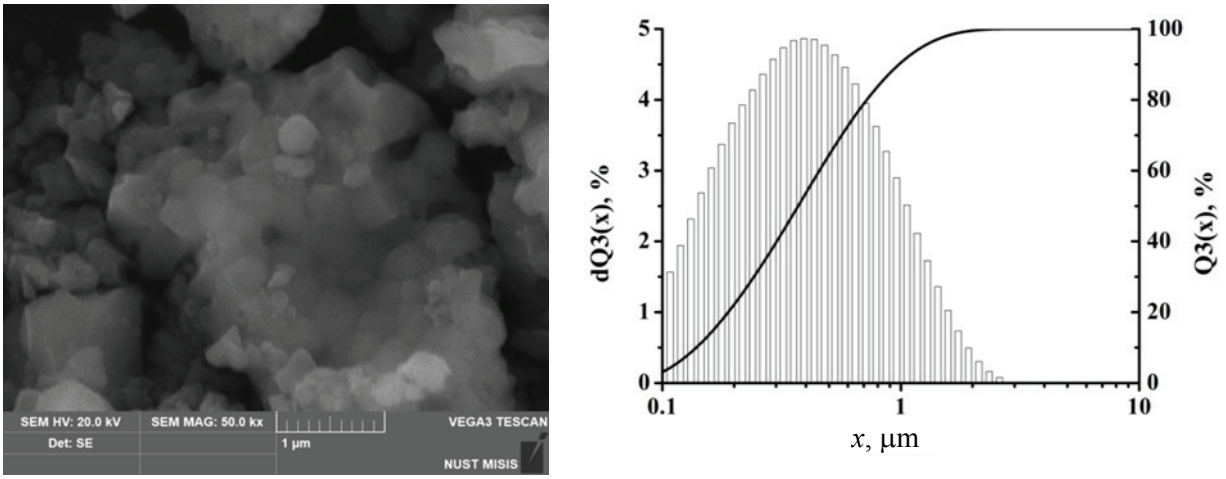

(*a* (*b*)

Fig. 2. SEM micrography and particle size distribution for nanopowders KFTO (*x* is particle size, μm; dQ3(*x*) is differential percentage of particle volume entering the range between the minimum and maximum size; Q3(*x*) is integral percentage of the particle volume relevant to the range in question, showing which fraction of the particle volume is below the specified size)

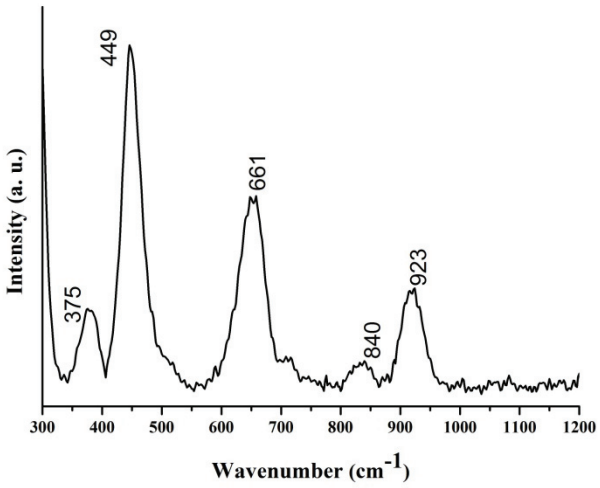

Fig. 3. Raman scattering spectra of priderite powder KFTO

These Ar-symmetry vibrations arising due to splitting of degenerate TiO_6 octahedron modes refer to the Ramman bands at 449 and 270 cm^{-1} [34]. The 661 cm^{-1} band can determine the titanium oxygen vibrations and the 840 cm^{-1} band probably corresponds to the valence vibrations of $(Fe,Ti)O_6$ octahedrons [35]. The 923 cm^{-1} band refers to the stretching vibrations of the Ti–O bonds including the unbound oxygen that K^+ ion coordinates with.

The electrical properties of the KFTO-based ceramics were studied in the frequency range of 10^{-1}–10^6 Hz at the room temperature. Figure 4 shows the frequency dependence of permittivity (ε′), dielectric losses (tan δ) and conductivity (σ) for a ceramic disks sintered at 1080 °C. The permittivity values show a tendency to decrease with increasing frequency (Fig. 4*a*), which is a characteristic property of polar dielectric materials. This feature is independent of the composition and stoichiometry of such materials. The displayed trend can be understood using the Wagner's theory. As can be seen, the resulting ceramics has high permittivity in the region of low frequencies ($\varepsilon' = 2.3 \cdot 10^4$). In the range of medium frequencies (1 kHz) $\varepsilon' = 2.6 \cdot 10^3$, and at high frequencies ε' decreases down to $7 \cdot 10^2$. It should be noted that traditionally the dielectric permittivity consists of three main components: the dipole grain (electronically anchored defective dipole); the grain interface (internal layer capacitance barrier); and the effect of electrode polarization [31]. At high frequencies ($f > 10^5$ Hz), permittivity occurs only due to the grain effect; at medium frequencies ($10 < f < 10^5$), the grain effect contribution is accompanied with a grain boundary effect corresponding to the IBLC model; while the electrode polarization effect occurs at low frequencies ($f < 10$). The high permittivity should be associated with the formation of either thin oxide films or secondary phases at the grain boundaries. In our study, Fe_2TiO_5 can be considere as a secondary phase. Thus, a structure represented by semiconducting grains and insulating grain boundaries characterized by increased polarizability and high value of ε′ can be formed. The high polarizability of the synthesized material may be explained by relatively high mobility of K^+ ions in the tunnel of the considered hollandite-like structure, accompanied by the redistribution of electrons in the crystalline titanate lattice through the $(Ti^{4+} \leftrightarrow Ti^{3+} - e^-)$ and $(Fe^{3+} \leftrightarrow Fe^{2+} - e^-)$ processes. The electrical conductivity of the tested

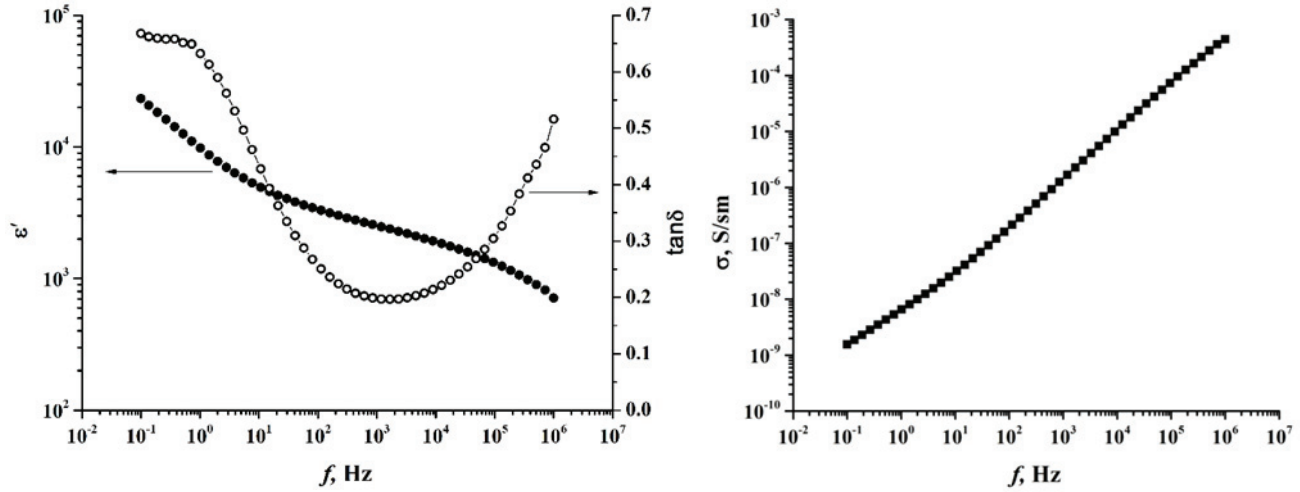

(*a*) (*b*)

Fig. 4. Frequency dependence of the real part of complex permittivity (ε′) and dielectric losses (tan δ) (*a*) conductivity (σ) (*b*) for the obtained ceramics

specimens increases with frequency and has high values for the ceramic materials in the low frequency range of $1.5 \cdot 10^{-9}$, and $4.5 \cdot 10^{-3}$ S·cm^{-1} in the high frequency range. This one indicates a presence of the potential barrier, which can be related to the boundary among the grains [32, 33].

As shown in Fig. 5 impedance hodographs have a typical appearance with small arcs and large arcs corresponding to high-frequency and low-frequency regions, respectively. The parallel appearance of small and large arcs indicates that a heterogeneous structure is formed in the sintered ceramic. The equivalent electric scheme consists of the following elements (Fig. 5): R_1, which describes the total resistance of contacts and wires, is not involved in the analysis. R_2 of the crystallite volume and grain boundaries, and the cascade connected in parallel consisting of resistance (grain boundary resistance); and constant phase elements CPE_1 has an index n_1 with a value close to 1, which allows it to be interpreted as capacity. In this case the value of CPE_1 10^{-9}, which is comparable to the grain boundary capacitance [36] and CPE_2 in turn has an index n_2 close to 0.5, which is interpreted as the impedance diffusion element whose value is presented in Table 1. An impedance study showed that the charge transfer in the studied sample is limited by barriers at the grain boundary and diffusion of charge carriers, which describe processes of charge transfer along the grain boundaries [37]. The calculated parameters of the equivalent circuit are presented in Table 1.

Two semicircles and a straight line with a certain slope angle are apparent in the Cole-Cole diagram (Fig. 6) for the dielectric permittivity. This indicates the presence of two relaxation processes as well as the contribution of the different components to the dielectric permittivity value, which can be determined using the adapted Gavriliak–Negami equation [38]:

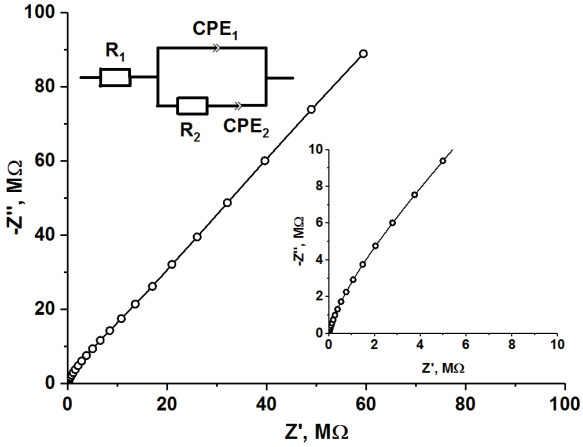

Fig. 5. The impedance spectroscopy (Nyquist plot) of KFTO-based ceramics measured at room temperature

Table 1. The values of the equivalent impedance circuit elements

Parameters	Value
R_1, Ω	75.85
R_2, Ω	20 300 000
CPE_1, nF	4.8
n_1	0.851
CPE_2, GΩ^{-1} s^n	9.14
n_2	0.579

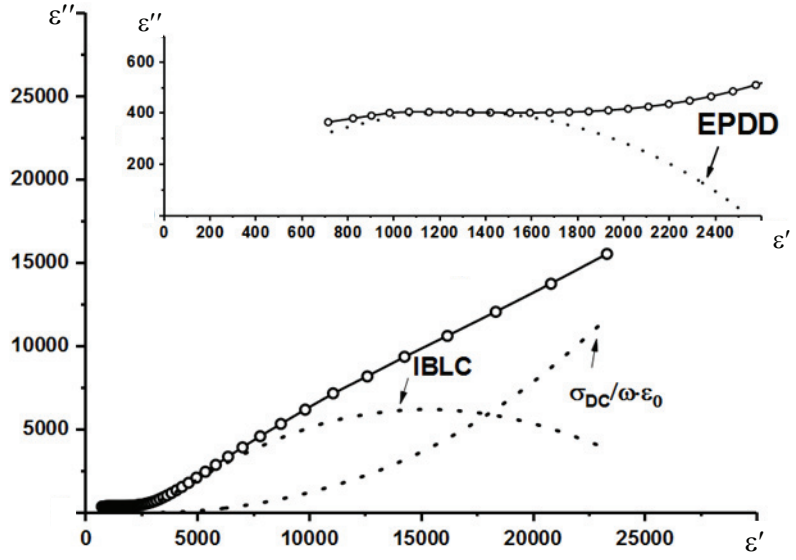

Fig. 6. Illustration of Cole-Cole model for KFTO-based ceramics

$$\varepsilon^* = \left(\varepsilon_\infty + \frac{\varepsilon_s - \varepsilon_\infty}{\left[1 + (j\omega\tau)^{1-\alpha}\right]^\beta} \right)_{\text{EPDD}} + \left(\varepsilon_\infty + \frac{\varepsilon_s - \varepsilon_\infty}{\left[1 + (j\omega\tau)^{1-\alpha}\right]^\beta} \right)_{\text{IBLC}} + \frac{j\sigma_{\text{DC}}}{\omega\varepsilon_0}, \quad (1)$$

where ε^* is the complex dielectric constant, ε_∞ is the permittivity at very high frequencies, ε_s is the static permittivity (low frequency permittivity values), $\omega = 2\pi f$ is the angular frequency, τ is the mean relaxation time, the exponent $(1 - \alpha)$ is a measure of the symmetric distribution of relaxation times, β is a measure of the asymmetrical distribution of relaxation times. The indices mean the contribution of dipolar grain (EPDD) and interfacial grain boundary (IBLC) to the permittivity value, respectively. Analysis of the Cole-Cole plot allowed us to determine the parameters of equation (1), which are summarized in Table 2.

Table 2. Eduation (1) parameters

Parameter	EPDD	IBLC
ε_s	2543.45	22432.64
ε_∞	50	2626.39
α	0.597	0
β	1	0.440
τ, s	$1.47 \cdot 10^{-9}$	0.908

Based on equation (1), Fig. 6 shows the multiple contributions of EPDD, IBLC and DC conductivity to the permittivity for KFTO ceramics. Based on this, the following assumptions can be made: the permittivity at high frequencies (10^6 Hz) consists only of the grain effect contribution (EPDD model); the dielectric constant at medium frequencies is determined by the contribution from grain and intergranular boundaries (IBLC), and in the low frequency region the contribution from crystal structure and microstructure as well as macro-interference between the metal electrode and heterogeneous ceramics is reflected. Calculated values of the elements of the equivalent impedance circuit for ceramic materials, confirm the presence of the above-mentioned processes. The equivalent circuit is represented by a two-series array of parallel RC (resistor and capacitor) elements. One of which contains the resistance R_1 characteristic of semiconductor grains. The other (consisting of resistance R_2 and CPE) represents the boundaries of insulating grains.

It is worth noting that the electrical properties of the hollandite synthesized in this study by the sol-gel method differ markedly from the properties of hollandite-like materials doped with other metals [19, 20]. The frequency dependence of conductivity is almost linear, with low values of σ_{dc} in the low-frequency area. Based on this one, it can be assumed that the changing the grain size and/or the doping the hollandite structure with other transition metal ions and will allow to adjust the electrical properties of the ceramic products. In addition, according to the literature data, KFTO ceramics has values of

permittivity and dielectric losses similar to these ones for the perovskite-like dielectrics. That makes it possible to propose to use this material with a hollandite-like structure in the producing of ceramic capacitors and other electronic components.

4. Conclusions

In this paper, we studied powder material with hollandite-like structure and composition $K_{1.6}Fe_{1.6}Ti_{6.4}O_{16}$ obtained by the Pechini method, successfully optimized for obtaining a single-phase solid solution in the system K_2O–Fe_2O_3–TiO_2 during heat treatment at 900 °C for 20 minutes, as well as ceramics based on it after compacting and sintering at 1080 °C. The XRD analysis showed the formation of the tetragonal hollandite phase with the spatial symmetry group l4/m. Apart from the hollandite phase, no other impurity phases were detected, which confirms the high degree of control of stoichiometry and purity using the Pechini method. To determine the structural characteristics of the obtained solid solution representing interconnected $(Fe,Ti)O_6$ octahedrons forming a frame structure with the tunnels filled with K^+ ions, the Rietveld method was applied, according to which the calculated parameters of the tetragonal crystal lattice were $a = b = 10.151$ Å and $c = 2.9659$ Å. The use of SEM and laser diffraction methods made it possible to analyze the size and morphology of the particles obtained by the Pechini method. It was found that the powder structure is formed by particles with uncertain morphology and an average size of 400 nm. It was found that powder with the hollandite structure during sintering melts incongruently with the formation of TiO_2 and Fe_2TiO_5 phases at the grain boundary. The dielectric properties of the $K_{1.6}Fe_{1.6}Ti_{6.4}O_{16}$ based ceramics measured by impedance spectroscopy allowed analyzing the frequency dependence of the real part of permittivity, dielectric losses and conductivity. The studied ceramics are characterized by high permittivity (especially in low-frequency region). In the middle frequency range (1 kHz) permittivity ε' and dielectric losses ($\tan\delta$) values are of $2.6 \cdot 10^3$ and 0.2, respectively. The obtained results enable to recommend using the hollandite-like ceramic materials in manufacturing of various ceramic elements of electronic devices, as well as fillers for polymer matrices due to their huge permittivity and specific frequency dependence of the electrical properties.

5. Funding

The research was funded by the Russian Scientific Foundation (contract No. 19-73-10133).

6. Conflict of interests

The authors declare no conflict of interest.

References

1. Yang L, Kong X, Li F, Hao H, Cheng Z, Liu H, Zhang S. Perovskite lead-free dielectrics for energy storage applications. *Progress in Materials Science*. 2019;102:72-108. DOI:10.1016/j.pmatsci.2018.12.005

2. Otitoju TA, Okoye PU, Chen G, Li Y, Okoye MO, Li S. Advanced ceramic components: Materials, fabrication, and applications. *Journal of Industrial and Engineering Chemistry*. 2020;85:34-65. DOI:10.1016/j.jiec.2020.02.002

3. Tian Z, Wang X, Shu L, Wang T, Song TH, Gui Z, Li L. Preparation of nano $BaTiO_3$-based ceramics for multilayer ceramic capacitor application by chemical coating method. *Journal of the American Ceramic Society*. 2009;92(4):830-833. DOI:10.1111/j.1551-2916.2009.02979.x

4. He Y, Zhang T, Zheng W, Wang R, Liu X, Xia Y, Zhao J. Humidity sensing properties of $BaTiO_3$ nanofiber prepared via electrospinning. *Sensors and Actuators B: Chemical*. 2010;146(1):98-102. DOI:10.1016/j.snb.2010.02.030

5. Supancic P. Mechanical stability of $BaTiO_3$-based PTC thermistor components: experimental investigation and theoretical modelling. *Journal of the European Ceramic Society*. 2000;20(12):2009-2024. DOI:10.1016/S0955-2219(00)00100-X

6. Zhu C, Zhao Q, Cai Z, Guo L, Li L, Wang X. High reliable non-reducible ultra-fine $BaTiO_3$-based ceramics fabricated via solid-state method. *Journal of Alloys and Compounds*. 2020;829:154496. DOI:10.1016/j.jallcom.2020.154496

7. Kishi H, Mizuno Y, Chazono H. Invited review paper-base-metal electrode-multilayer ceramic capacitors: past, present and future perspectives. *Japanese Journal of Applied Physics-Part 1 Regular Papers and Short Notes*. 2003;42(1):1-15. DOI:10.1143/JJAP.42.1

8. Wang CM, Kao KS, Lin SY, Chen YC, Weng SC. Processing and properties of $CaCu_3Ti_4O_{12}$ ceramics. *Journal of Physics and Chemistry of Solids*. 2008;69(2-3):608-610. DOI:10.1016/j.jpcs.2007.07.049

9. Zhang J, Zheng J, Liu Y, Zhang C, Hao W, Lei Z, Tian M. The dielectric properties of CCTO ceramics prepared via different quick quenching methods. *Materials Research Bulletin*. 2019;115:49-54. DOI:10.1016/j.materresbull.2019.03.006

10. Jumpatam J, Putasaeng B, Chanlek N, Manyam J, Srepusharawoot P, Krongsuk S. Thongbai P. Influence of Sn and F dopants on giant dielectric response and Schottky potential barrier at grain boundaries of CCTO ceramics. *Ceramics International*. 2021;47(19):27908-27915. DOI:10.1016/j.ceramint.2021.06.221

11. Shanmugasundram HPPV, Jayamani E, Soon KH. A comprehensive review on dielectric composites: Classification of dielectric composites. *Renewable and Sustainable Energy Reviews*. 2022;157:112075. DOI: 10.1016/j.rser.2022.112075

12. Moetakef P, Larson AM, Hodges BC, Zavalij P, Gaskell KJ, Piccoli PM, Rodriguez EE. Synthesis and crystal chemistry of microporous titanates $K_x(Ti,M)_8O_{16}$ where M = Sc – Ni. *Journal of Solid State Chemistry*. 2014;220:45-53. DOI:10.1016/j.jssc.2014.08.012

13. Usman M, Kocevski V, Smith MD, Morrison G, Besmann T, Loye HCZ. New rubidium-containing mixed-metal titanium hollandites. *Crystal Growth & Design*. 2020;20(4):2398-2405. DOI:10.1021/acs.cgd.9b01560

14. Tumurugoti P, Betal S, Sundaram SK. Hollandites' crystal chemistry, properties, and processing: a review. *International Materials Reviews*. 2021;66(3): 141-159. DOI:10.1080/09506608.2020.1743592

15. Krishna SR, Shrujana P, Palla S, Sreenu K, Velchuri R, Vithal M. Preparation, characterization and photocatalytic studies of $K_2Al_2Ti_6O_{16}$, $K_{2-x}Ag_xAl_2Ti_6O_{16}$ and $K_2Al_2Ti_6O_{16-x}N_y$. *Materials Research Express*. 2015;2(3):035008. DOI: 10.1088/2053-1591/2/3/035008

16. Knyazev AV, Chernorukov NG, Ladenkov IV, Belopol'skaya SS. Synthesis, structure, and thermal expansion of $M_2Fe_2Ti_6O_{16}$ and $MFeTiO_4$ compounds. *Inorganic Materials*. 2011;47(9):999-1005. DOI:10.1134/S0020168511090123

17. Kijima N, Sakao M, Manabe T, Akimoto J. Synthesis, crystal structure, and electrochemical properties of niobium-substituted hollandite-type titanium dioxides, $K_xTi_{1-y}Nb_yO_2$, with different potassium content in the tunnel space. *Solid State Ionics*. 2021;369:115727. DOI: 10.1016/j.ssi.2021.115727

18. Ma J, Fang Z, Yang X, Wang B, Luo F, Zhao X, Yang Y. Investigating hollandite–perovskite composite ceramics as a potential waste form for immobilization of radioactive cesium and strontium. *Journal of Materials Science*. 2021;56(16):9644-9654. DOI:10.1007/s10853-021-05886-2

19. Gorshkov N, Vikulova M, Gorbunov M, Mikhailova D, Burmistrov I, Kiselev N, Gorokhovsky A. Synthesis of the hollandite-like copper doped potassium titanate high-k ceramics. *Ceramics International*. 2021; 47(4):5721-5729. DOI:10.1016/j.ceramint.2020.10.158

20. Gorokhovsky AV, Tretyachenko EV, Goffman VG, Gorshkov NV, Fedorov FS, Sevryugin AV. Preparation and dielectric properties of ceramics based on mixed potassium titanates with the hollandite structure. *Inorganic Materials*. 2016;52(6):587-592. DOI:10.1134/S0020168516060042

21. Vikulova M, Tsyganov A, Bainyashev A, Artyukhov D, Gorokhovsky A, Muratov D, Gorshkov N. Dielectric properties of PMMA/KCTO (H) composites for electronics components. *Journal of Applied Polymer Science*. 2021;138(40):51168. DOI:10.1002/app.51168

22. Liu T, Li Q, Xin Y, Zhang Z, Tang X, Zheng L, Gao PX. Quasi free K cations confined in hollandite-type tunnels for catalytic solid (catalyst)-solid (reactant) oxidation reactions. *Applied Catalysis B: Environmental*. 2018;232:108-116. DOI:10.1016/j.apcatb.2018.03.049

23. Zaitouni H, Hajji L, Mezzane D, Choukri E, Alimoussa A, Moumen SB, Rožič B, El Marssi M, Kutnjak Z. Direct electrocaloric, structural, dielectric, and electric properties of lead-free ferroelectric material $Ba_{0.9}Sr_{0.1}Ti_{1-x}Sn_xO_3$ synthesized by semi-wet method. *Physica B: Condensed Matter*. 2019;566:55-62. DOI:10.1016/j.physb.2019.04.026

24. Morozov NA, Sinelshchikova OY, Besprozvannykh NV, Ugolkov VL. Citrate-nitrate synthesis and the electrophysical properties of ceramics in the $K_2O–TiO_2–Fe_2O_3$ system. *Glass Physics and Chemistry*. 2021;47(5):481-488. DOI:10.1134/S1087659621050114

25. Morozov NA, Sinelshchikova OY, Besprozvannykh NV, Maslennikova TP. Effect of the method of synthesis on the photocatalytic and sorption properties for potassium polytitanates doped with di-and trivalent metal ions. *Russian Journal of Inorganic Chemistry*. 2020;65(8):1127-1134. DOI:10.1134/S0036023620080124

26. Besprozvannykh NV, Sinel'shchikova OY, Morozov NA, Kuchaeva SK, Postnov AY. Synthesis and physicochemical properties of complex oxides $K_2Me_xTi_{8-x}O_{16}$ (Me = Mg,Ni,Al) of hollandite structure. *Russian Journal of Applied Chemistry*. 2020;93(8):1132-1138. DOI:10.1134/S1070427220080042

27. Hassan QU, Yang D, Zhou JP, Lei YX, Wang JZ, Awan SU. Novel single-crystal hollandite $K_{1.46}Fe_{0.8}Ti_{7.2}O_{16}$ microrods: synthesis, double absorption, and magnetism. *Inorganic Chemistry*. 2018;57(24):15187-15197. DOI: 10.1021/acs.inorgchem.8b02481

28. Caminata LP, Perdomo CP, Kiminami RH. Effect of microwave heating during evaporation solvent and polymeric precursor formation in synthesis of $BaZr_{0.08}Ti_{0.92}O_3$ nanopowders. *Journal of Solid State Chemistry*. 2020;291:121586. DOI:10.1016/j.jssc.2020.121586

29. Fang P, Xi Z, Long W, Li X, Qiu S. Synthesis and dielectric properties of the Aurivillius oxide $BaBi_4Ti_4O_{15}$ by the Pechini method. *Journal of Sol-Gel Science and Technology*. 2014;71(2):241-245. DOI:10.1007/s10971-014-3363-z

30. Mastoroudes BC, Markgraaff J, Wagener JB, Olivier EJ. Synthesis of cesium, sodium and nitrogen derived titanates using the Pechini sol-gel method. *Chemical Physics*. 2020;537:110816. DOI:10.1016/j.chemphys.2020.110816

31. Tuichai W, Danwittayakul S, Srepusharawoot P, Thongbai P, Maensiri S. Giant dielectric permittivity and electronic structure in (A^{3+}, Nb^{5+}) co-doped TiO_2 (A = Al, Ga and In). *Ceramics International*. 2017;43:S265-S269. DOI:10.1016/j.ceramint.2017.05.255

32. Felix AA, Orlandi MO, Varela JA. Schottky-type grain boundaries in CCTO ceramics. *Solid State Communications*. 2011;151(19):1377-1381. DOI:10.1016/j.ssc.2011.06.012

33. Costa SI, Li M, Frade JR, Sinclair DC. Modulus spectroscopy of $CaCu_3Ti_4O_{12}$ ceramics: clues to the internal

barrier layer capacitance mechanism. *RSC Advances*. 2013;3(19):7030-7036. DOI:10.1039/C3RA40216A

34. Gao T, Fjellvag H, Norby P. Raman scattering properties of a protonic titanate $H_xTi_{2-x/4}$ square $O_{x/4}$ (4) center dot H_2O (square, vacancy; $x = 0.7$) with lepidocrocite-type layered structure. *Journal of Physical Chemistry B*. 2008;112(31):9400-9405. DOI:10.1021/jp801639a

35. Knyazev AV, Mączka M, Ladenkov IV, Bulanov EN, Ptak M. Crystal structure, spectroscopy, and thermal expansion of compounds in $MI_2O–Al_2O_3–TiO_2$ system. *Journal of Solid State Chemistry*. 2012;196:110-118. DOI:10.1016/j.jssc.2012.05.043

36. Barsoukov E, Macdonald JR. *Impedance spectroscopy theory, experiment and applications*, 2nd ed. Hoboken, NJ: John Wiley &Sons, Inc.; 2005. 595 p.

37. West AR, Adams TB, Morrison FD, Sinclair DC. Novel high capacitance materials:-$BaTiO_3$: La and $CaCu_3Ti_4O_{12}$. *Journal of the European Ceramic Society*. 2004;24(6):1439-1448. DOI:10.1016/S0955-2219(03)00510-7

38. Jana PK, Sarkar S, Karmakar S, Chaudhuri BK. Conduction mechanism and dielectric relaxation in high dielectric $K_xTi_yNi_{1-x-y}O$. *Journal of Applied Physics*. 2007;102(8):084105. DOI:10.1063/1.2799071

Информация об авторах / Information about the authors

Алексей Русланович Цыганов, младший научный сотрудник, ФГБОУ ВО «Саратовский государственный технический университет имени Гагарина Ю.А.» (СГТУ имени Гагарина Ю.А.), Саратов, Российская Федерация; ORCID 0000-0002-5112-7939; e-mail: tsyganov.a.93@mail.ru

Александр Владиленович Гороховский, доктор химических наук, профессор, заведующий кафедрой «Химия и химическая технология материалов», СГТУ имени Гагарина Ю.А., Саратов, Российская Федерация; ORCID 0000-0002-4210-3169; e-mail: Algo54@mail.ru

Мария Александровна Викулова, кандидат химических наук, доцент, старший научный сотрудник, СГТУ имени Гагарина Ю.А., Саратов, Российская Федерация; ORCID 0000-0003-0092-6922; e-mail: vikulovama@yandex.ru

Денис Иванович Артюхов, аспирант СГТУ имени Гагарина Ю.А., Саратов, Российская Федерация; ORCID 0000-0001-9753-8875; e-mail: mr.tokve@gmail.com

Дмитрий Альбертович Захарьевич, кандидат физико-математических наук, доцент, ФГБОУ ВО «Челябинский государственный университет», Челябинск, Российская Федерация; ORCID 0000-0003-1184-9571; e-mail: dmzah@csu.ru

Светлана Ивановна Саунина, кандидат физико-математических наук, доцент, ФГБОУ ВО «Челябинский государственный университет», Челябинск, Российская Федерация; ORCID 0000-0003-1274-7032; e-mail: sauninasi@mail.ru

Николай Вячеславович Горшков, кандидат технических наук, доцент, старший научный сотрудник, СГТУ имени Гагарина Ю.А., Саратов, Российская Федерация; ORCID 0000-0003-3248-3257; e-mail: gorshkov.sstu@gmail.com

Alexey R. Tsyganov, Junior Researcher, Yuri Gagarin State Technical University of Saratov (SSTU), Saratov, Russian Federation; ORCID 0000-0002-5112-7939; e-mail: tsyganov.a.93@mail.ru

Alexander V. Gorokhovsky, D. Sc. (Chemistry), Professor, Head of the Department «Chemistry and Chemical Technology of Materials», SSTU, Saratov, Russian Federation; ORCID 0000-0002-4210-3169; e-mail: Algo54@mail.ru

Maria A. Vikulova, Cand. Sc. (Chemistry), Associate Professor, Senior Researcher, SSTU, Saratov, Russian Federation; ORCID 0000-0003-0092-6922; e-mail: vikulovama@yandex.ru

Denis I. Artyukhov, Postgraduate, SSTU, Saratov, Russian Federation; ORCID 0000-0001-9753-8875; e-mail: mr.tokve@gmail.com

Dmitry A. Zakharievich, Cand. Sc. (Physics and Mathematics), Associate Professor, Chelyabinsk State University, Chelyabinsk, Russian Federation; ORCID 0000-0003-1184-9571; e-mail: dmzah@csu.ru

Svetlana I. Saunina, Cand. Sc. (Physics and Mathematics), Associate Professor, Chelyabinsk State University, Chelyabinsk, Russian Federation; ORCID 0000-0003-1274-7032; e-mail: sauninasi@mail.ru

Nikolay V. Gorshkov, Cand. Sc. (Engineering), Associate Professor, Senior Researcher, SSTU, Saratov, Russian Federation; ORCID 0000-0003-3248-3257; e-mail: gorshkov.sstu@gmail.com

Received 24 December 2021; Accepted 18 February 2022; Published 14 April 2022